Molecular Catalysis 479 (2019) 110632

Contents lists available at ScienceDirect

Molecular Catalysis

journal homepage: www.elsevier.com/locate/mcat

A facile way for sugar transformation catalyzed by carbon-based Lewis-Brønsted solid acid

Surachai Karnjanakom[a,*], Panya Maneechakr[a,*], Chanatip Samart[b], Guoqing Guan[c]

[a] Department of Chemistry, Faculty of Science, Rangsit University, Pathumthani 12000, Thailand
[b] Department of Chemistry, Faculty of Science and Technology, Thammasat University, Pathumthani 12120, Thailand
[c] Energy Conversion Engineering Group, Institute of Regional Innovation (IRI), Hirosaki University, 2-1-3, Matsubara, Aomori 030-0813, Japan

ARTICLE INFO

Keywords:
Sugar
EMF
SO_3H-Zn-SC
Ultrasonic
Selectivity

ABSTRACT

In this work, catalytic transformation of sugar into 2-Formyl-5-ethoxymethylfuran (EMF) was studied using Zn-trapped sulfonated carbon (SO_3H-Zn-SC) catalyst. The catalyst was easily prepared via impregnation-pyrolysis and sulfonation. The physical and chemical properties of as-prepared catalyst were tested and discussed in details. For upgrading experiment, EMF synthesis from glucose transformation via isomerization, dehydration and etherification processes was performed using ultrasonic system. The increasing of ultrasonic power and ultrasonic duty cycle promoted the formation of EMF product, providing a maximum EMF yield of 97.8%. The ultrasonic application promoted the selectivity for EMF formation at shorter-faster reaction rate. Moreover, SO_3H-Zn-SC also exhibited good reusability with low amount of acid leaching in each cycle. This research provided alternative way for improving the yield of EMF at short reaction time.

Introduction

Biomass and carbohydrate are selected as an alternative way to solve the problem of energy crisis since it can be converted into biofuel, chemical building blocks and additive petroleum fuels by several technologies in the past few years [1,2]. 2-Formyl-5-ethoxymethylfuran (EMF) is identified as a liquid biofuel candidate for application in energy industrial process because its energy density property is close to diesel [3]. This chemical can be produced from conversion of sugars through isomerization, dehydration or etherification in the presence of water, ethanol and acid catalysts. In general, strong acids such as hydrochloric acid and sulfuric acid have been utilized as homogeneous acid catalysts for EMF production in industrial process. Recently, it is clearly reported that Lewis-acid catalyst such as chromium chloride had specific performance for catalytic conversion glucose into fructose [4]. More interestingly, the synergistic effect of 1-Butyl-3-methylimidazolium chloride (BMIMCl) ionic liquid with aluminum chloride well served for EMF formation under hydrothermal system with high pressure [5,6]. Unluckily, the application of homogeneous system based on above literatures resulted in the occurrence of serious drawbacks such as large amounts of impurities and sewage in EMF product. Moreover, EMF separation/purification processes are quite difficulty, leading to high production cost [7,8]. Heterogeneous catalysts have been applied to solve above drawbacks. Liu et al [9] found that A 83.4% of EMF yield was obtained from HMF conversion via etherification reaction catalyzed by mesoporous MCM-41 supported 12-tungstophosphoric acid. Morales et al. [10] synthesized the arenesulfonic acid-modified SBA-15 mesostructured silica (Ar-SO_3H-SBA-15), and applied for catalyzing in transformation of fructose in co-solvent (ethanol + dimethylsulfoxide) to produce EMF. They found that EMF yield of 63.4% could be achieved at 116 °C for 4 h using Ar-SO_3H-SBA-15 catalyst. Wang et al. [11] reported that the catalytic production of EMF over acid-functionalized ordered mesoporous carbon (OMC-SO_3H) at 140 °C for 24 h, providing EMF yields of 55.7%, 53.6% and 26.8% from fructose, iuline and sucrose, respectively. Howsoever, there are some issue that is necessary to be solved at first. For example, too high reaction temperature and long reaction was conducted for EMF synthesis process with high product yield obtained. Also, as-mentioned heterogeneous catalysts have very expensive and quite a lot complicated to prepare, which limits further utilization in industrial process. In our ideas, it needs to search and develop new catalysts where are environmental available, low cost and better catalytic performance for EMF synthesis. Here, from economical point of view, we considered to apply carbon materials derived from biomass residue as heterogeneous catalyst [12–14].

Based on above introduction, the effective carbon catalyst was prepared by impregnation, pyrolysis and sulfonation processes. The wood residue obtained from wood processing plant was used as a carbon source. The properties of catalyst were investigated by N_2

* Corresponding authors.
E-mail addresses: surachai.ka@rsu.ac.th (S. Karnjanakom), panya.m@rsu.ac.th (P. Maneechakr).

https://doi.org/10.1016/j.mcat.2019.110632
Received 12 May 2019; Received in revised form 12 September 2019; Accepted 13 September 2019
Available online 24 September 2019
2468-8231/ © 2019 Elsevier B.V. All rights reserved.

sorption, XRD, SEM-EDS, titration and NH_3-TPD techniques. The experimental designs using 2^4 factorial design were carried out to find the significant levels of each factor and optimal conditions for synthesis of EMF from glucose transformation [15,16]. Various factors such as catalyst amount, reaction time, reaction temperature and ultrasonic power were systematically investigated at 95% confidence level. The turnover rate of glucose conversion into EMF was also studied together with catalyst reusability test for 5 cycles. This research provided alternative way for improving the yield of EMF at short reaction time using effective catalyst.

Experimental

Preparation of SO_3H-Zn-SC catalyst

10 g of wood residue was impregnated with a certain amount of 15 wt.% $ZnCl_2$ solution, and stirred for 12 h. Here $AlCl_3$ was also used to compare the activity with $ZnCl_2$. Then, it was heat at 80 °C for 6 h in order to eliminate water. The pyrolysis of impregnated wood was carried out at 650 °C for 2 h and followed by sulfonation process at 150 °C for 24 h using concentrated H_2SO_4. Here, the mass ratio of sample to H_2SO_4 (1–3) was selected to use in this study [17]. Thereafter, the obtained black powder or catalyst was filtered, washed with EtOH and DI water for several times in order to eliminate excess sulfate ions, and dried at 110 °C for 24 h. It should be noted that SC trapped with $ZnCl_2$ and functionalized with sulfonic group was denoted as SO_3H-Zn-SC catalyst.

Catalyst characterization

The BET surface area and pore size of catalyst were analyzed by N_2 adsorption-desorption analyzer. The XRD pattern of catalyst structure was recorded using an X-ray diffractometer in 2-theta range of 20-70° with a scanning step of 0.02°. The surface morphology of catalyst and the presence of S and Zn elements on catalyst were observed by a scanning electron microscope (SEM) equipped with energy dispersive spectroscopy (EDS). The acidity and acid amount of catalyst were investigated by NH_3-Temperature-programmed desorption (NH_3-TPD) and back titration, respectively [18]. Thermal stability of sulfonic group attached on catalyst surface was analyzed using a Thermogravimetric analyzer at conditions of 100–800 °C with heating rate of 5 °C/min under N_2 flow.

Catalytic performance testing for EMF production

The catalytic upgrading of glucose was carried out in a three-neck round bottom flask equipped with a reflux condenser and an ultrasonic probe as well as a thermocouple thermometer. In each experiment, a frequency of 40 kHz, a ultrasonic power of 80 W and a stirring speed at 600 rpm were applied. In a typical run, 0.5 g of glucose (Ajax Finechem), 20 mL of ethanol (99% Fisher BioReagents), 5 mL of distilled water, 1.5 g of NaCl (Ajax Finechem), 20 mL of tetrahydrofuran (99.9%, Sigma-Aldrich), and required amount of catalyst were added into reactor. Then, reaction was performed at 106 °C for 72 min based on our preliminary optimization. After finishing reaction, the mixture product was cooled in an ice-bath, diluted and filtered with syringe filter. Before reusability test, the spent catalyst was washed with DI water and acetone for several times to eliminate contaminant, and then dried for 24 h [19]. The glucose and EMF product were analyzed by an Agilent 1200 HPLC chromatograph equipped with an Aminex HPX-87H column as well as refractive index and UV detectors. 0.5 mM H_2SO_4 solution was utilized as mobile phase at column temperature of 60 °C with a total flow rate of 0.6 ml/min. The conversion of substrate and the selectivity of each product were determined using an external standard method, and calculated according to Eqs. (1) and (2):

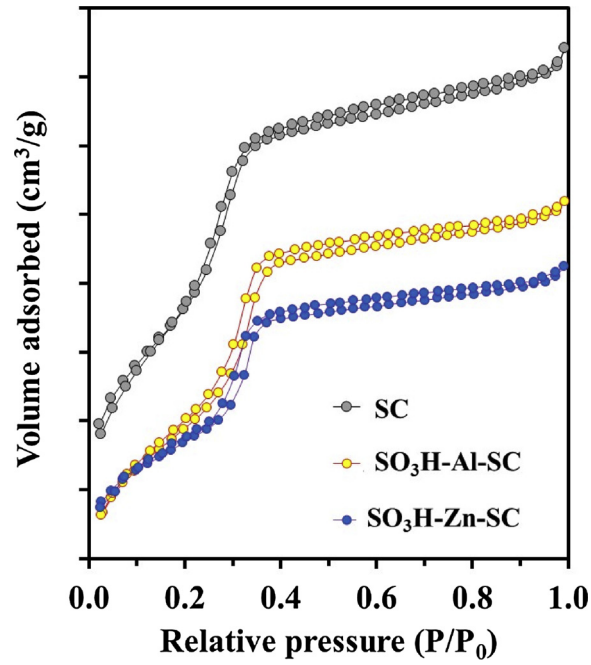

Fig. 1. N_2 sorption isotherms SC, SO_3H-Zn-SC and SO_3H-Al-SC.

$$\text{Glucose conversion (\%)} = \frac{\text{Mole percentage of glucose reacted}}{\text{Mole percentage of initial glucose}} \times 100 \quad (1)$$

$$\text{Product selectivity (\%)} = \frac{\text{Mole percentage of product produced}}{\text{Mole percentage of glucose reacted}} \times 100 \quad (2)$$

The details, including equations and examples of the mathematical method of experimental designs using 2^4 factorial of a system with 4 factors and 2 levels, "a screening design of low (-1) and high (+1)" as well as kinetic study are provided in supporting information (SI).

Results and discussion

Physical and chemical properties of SO_3H-Zn-SC catalyst

N_2 sorption isotherms of SC and SO_3H-Zn-SC are shown in Fig. 1. As observed, both samples exhibited the same pattern of type VI isotherms which had characteristic hysteresis loops, indicating to mesoporous structure with capillary condensation within uniform pores. [20]. Also, the apparent reduction in volume adsorbed was found for SO_3H-Zn-SC, comparing with SC without modification. This phenomenon could be described to the presence of sulfonic group and ZnO attached on the surface of catalyst. This result was in good agreement with Table 1 which presentd the textural properties of catalyst. The surface area and pore size of SC were decreased to some extent after modification process. The XRD pattern of catalysts are presented in Fig.2. The diffraction peaks for SC were appeared at 10-30° and 35–50 °C, suggesting to amorphous solid carbon structure [21]. After modification, the diffraction peak of SO_3H-Zn-SC were appeared at 2-theta of 31.8, 34.6, 36.3, 47.7, 56.7, 62.9, 66.6, 68.1, and 69.2° which should be attributed to ZnO crystal planes [22]. In case of $AlCl_3$ modification, the diffraction peak SO_3H-Al-SC presented broad crystalline peaks at 45 and 67∘ which could be ascribed to the reflections on (400) and(440) crystal planes of the γ-Al_2O_3 phase on SC.

The acid amounts of SC and SO_3H-Zn-SC and SO_3H-Al-SC derived from back titration were 2.26, 4.59 and 4.68 mmol/g, respectively (Table 1). The NH_3-TPD profiles of SO_3H-Zn-SC and SO_3H-Al-SC are presented in Fig. 3. It is found that Two NH_3 desorption peaks were appeared at low temperature (~228 °C) and high temperature

Table 1
Physical and chemical properties of catalysts.

Catalyst	Surface area[a] (m^2/g)	Pore volume[b] (cm^3/g)	Pore size[b] (nm)	Acid amount[c] (mmol/g)
SC	752	0.86	2.54	2.26
SO_3H-Zn-SC	543	0.69	2.22	4.59
Spent SO_3H-Zn-SC	538	0.68	2.13	4.55
SO_3H-Al-SC	586	0.73	2.03	4.68
Spent SO_3H-Al-SC	563	0.66	1.86	4.43

[a] BET method.
[b] BJH method.
[c] Back titration method.

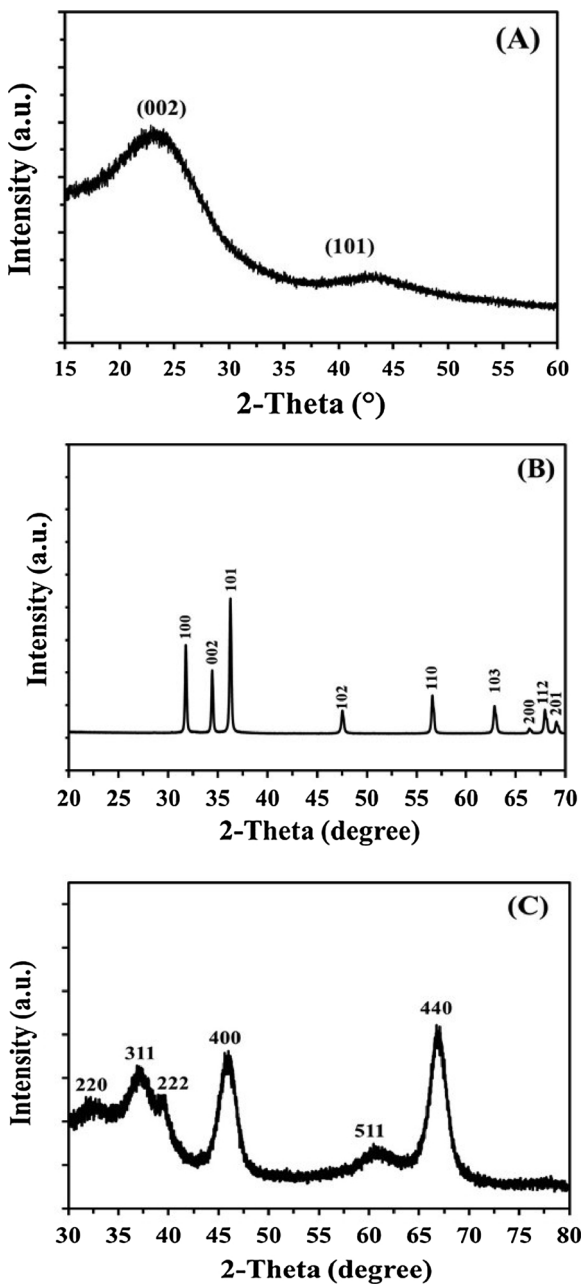

Fig. 2. (A,B) XRD patterns of (A) SC, (B) SO_3H-Zn-SC and (C) SO_3H-Al-SC.

(~417 °C) which could be attributed to the weak/Lewis acid and strong/Brönsted acid sites, respectively [23]. As observed, SO_3H-Al-SC presented the presence of stronger acid site with higher amount than NH_3 desorption of SO_3H-Zn-SC. This phenomenon should be resulted

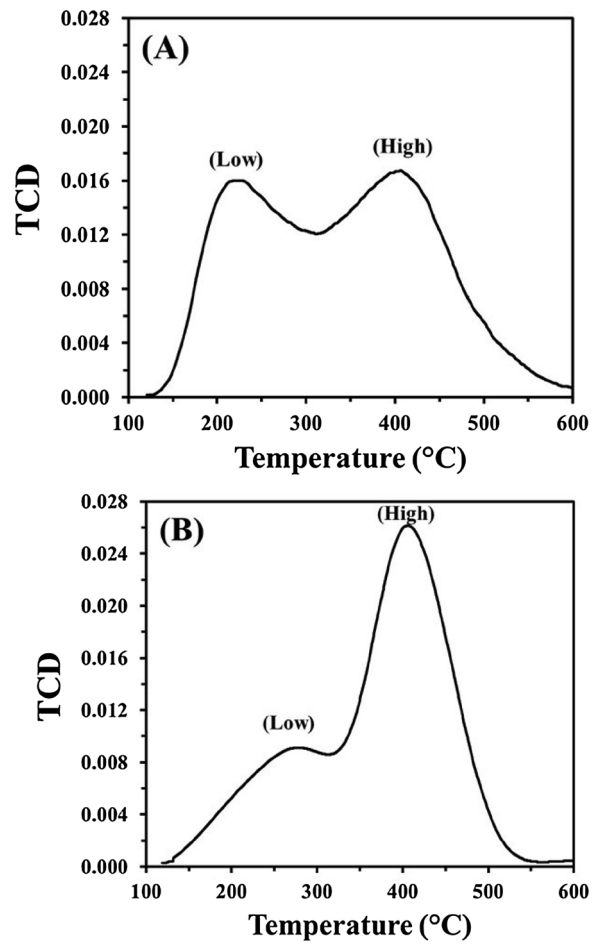

Fig. 3. NH_3-TPD profiles of (A) SO_3H-Zn-SC and (B) SO_3H-Al-SC.

from different kinds of metal elements as well as their interaction. Here, the high acid amount on catalyst consisted of Lewis and Bronsted acids should be resulted in promoting the reactions such as isomerization, dehydration and etherification processes for EMF formation. The SEM-EDS images of SO_3H-Zn-SC are shown in Fig. 4. As observed, the presence of Zn Al and S elements on SC structure was explicitly observed in SEM image. The EDS mapping could be confirmed that each element was well distributed on surface of SC support.

Catalytic transformation of glucose into EMF

The complete sixteen experiments with observed EMF yield under 2^4 factorial design is shown in Table S1 and Table S2. The discussion on details of this design are provided in SI. Here, the significant factor such as catalyst amount (25 to 75 g), reaction time (30 to 90 min), reaction temperature (80 to 120 °C) had significant results at 95% confidence level. As expected, highest F-value of catalyst amount was found to be

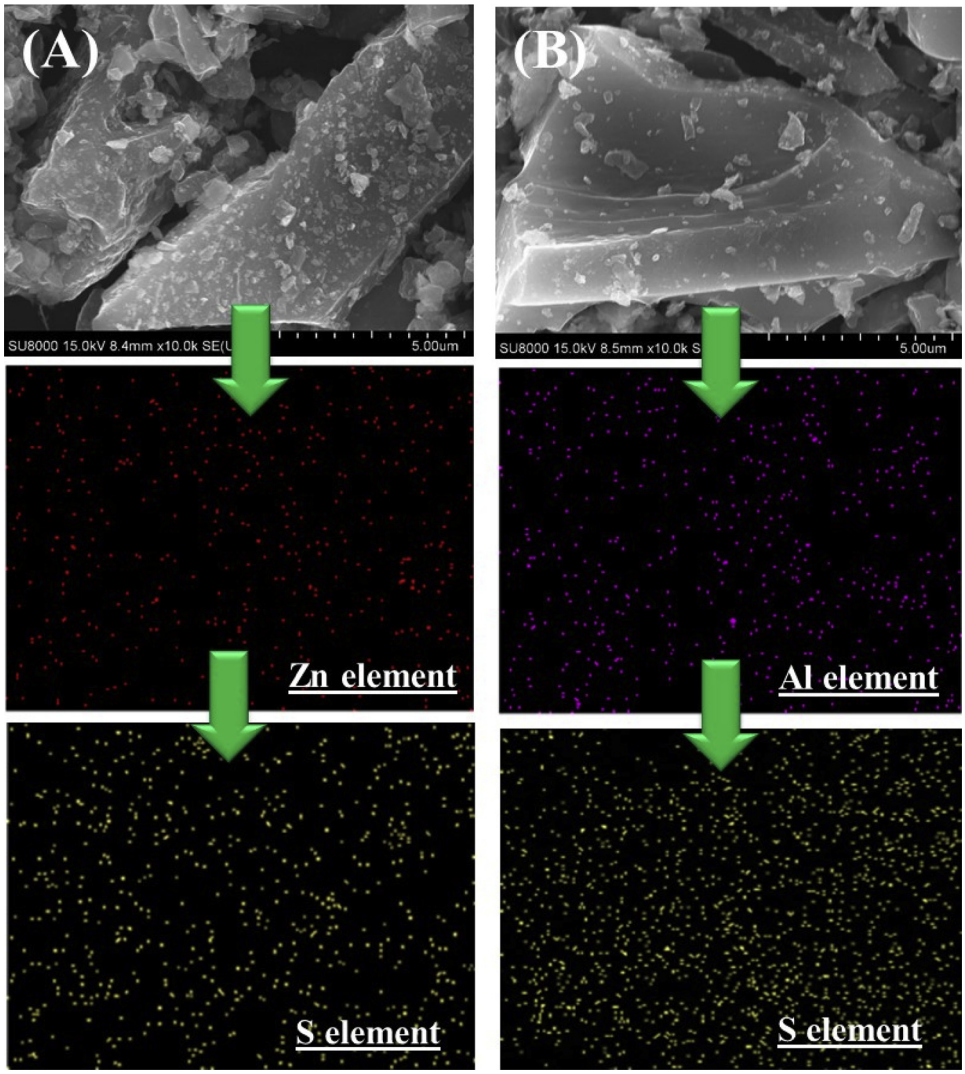

Fig. 4. SEM-EDS images of (A) SO_3H-Zn-SC and (B) SO_3H-Al-SC.

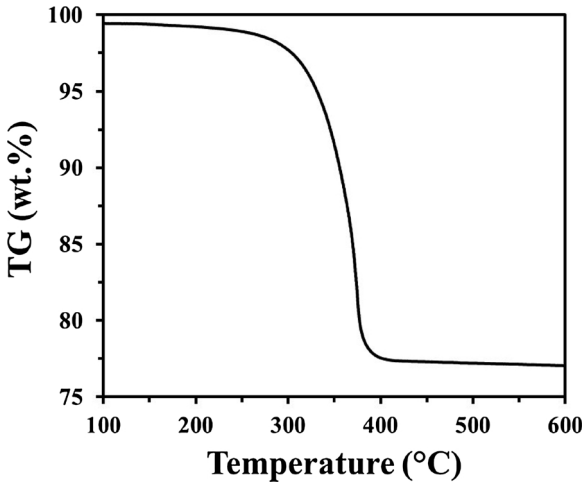

Fig. 5. TG profiles of SO_3H-Zn-SC.

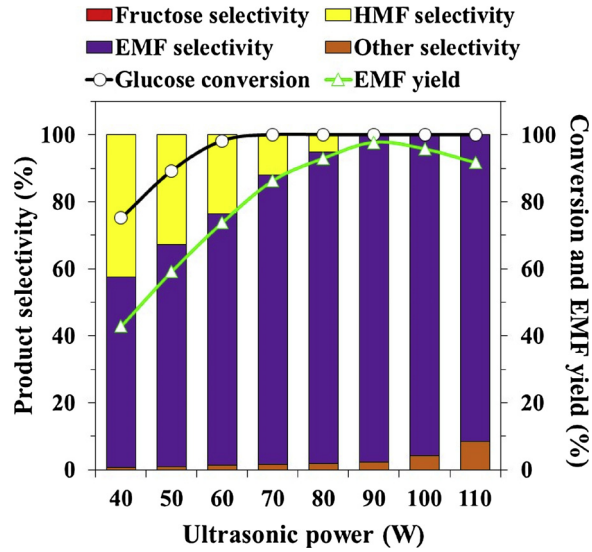

Fig. 6. Effect of ultrasonic power for transformation of glucose into EMF over SO_3H-Zn-SC at conditions: catalyst 62 mg, reaction time of 72 min, reaction temperature of 106 °C and THF amount of 250 mmol.

~2060, indicating to level of significant factor. The THF amount in the range applied had no influence on promoting the EMF yield, indicating that a lowest amount of 250 mmol was adequate for EMF production in this study. It should be noted that temperature range about 80 to 120 °C applied for EMF production had no effect for leaching of sulfonic group

attached on catalyst during reaction process. This could be confirmed in TGA results (Fig. 5). The thermal decomposition of sulfonic from SO_3H-Zn-SC was observed at temperature range of ~250-450 °C, suggesting that the as-prepared catalyst had high thermal stability at a temperature > 200 °C [24]. Fig. 6 shows the influence of ultrasonic power on glucose conversion into EMF products using SO_3H-Zn-SC. When ultrasonic power increased from 70 W to 90 W, a steady increase in the EMF yield from 86.3% to 97.8% could be observed, indicating that the higher ultrasonic power well promoted isomerization-dehydration-etherification of glucose. In the other words, an increase in ultrasonic power may be correlated with the number of cavitation bubbles formed in the medium, and therefore, promoting the EMF formation. This could also improve in assisting of the niche collapse which resulted in reduced energy transfer into the reaction system. Here, the advantage of ultrasonic technology could be summarized as follows: (I) shorter reaction time, lower reaction temperature and higher product yield were found when compared with conventional reflux/hydrothermal method, and (II) the unwanted products such as humins and carbons could be evidently obstructed. However, the yield of EMF was decreased while other side products were increased to some extent since too high ultrasonic power as over 90 W was applied. Thus, ultrasonic power (90 W) was selected as an optimum power dispersal. Fig. 7 shows the influence of ultrasonic duty cycle on glucose conversion into EMF products using SO_3H-Zn-SC. Here, ultrasonic duty cycle was defined by varying ON-OFF time of ultrasonic irradiation, for instance, a duty cycle of 40% was corresponding to ultrasonic irradiation for 4 s and followed by a rest period of 6 s (no ultrasonic irradiation). This utilization was expected to achieve the highest EMF yield as well as to recognize the appropriate increasing of ON time that would affect in unnecessary consumption of energy. One can see that the EMF yield was obviously increased from 12.8% to 97.8% with the increasing of duty cycle from 20% (2 s ON and 8 s OFF) to 70% (7 s ON and 3 s OFF) and after that there was no any significant changing for next increasing in the duty cycle until to 90% (9 s ON 1 s OFF). It should be noted that in the case conventional reflux system, it required the reaction time at least 6 h for obtaining the EMF yield (~98%). In this study, in-situ extraction of EMF from THF layer was succeeded, obtaining EMF up to > 99%. Also, to increase the immiscibility between EtOH/distilled water and THF, it was carried out by adding a small amount of NaCl into the system. The two layer of mixture solution was finally obtained. (Fig. S3). The possible mechanism for catalytic upgrading of glucose into EMF are

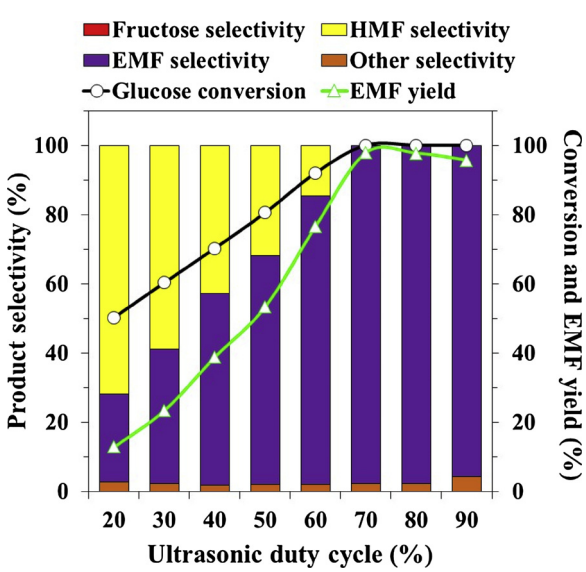

Fig. 7. Effect of ultrasonic duty cycle for transformation of glucose into EMF over SO_3H-Zn-SC at conditions: catalyst 62 mg, reaction time of 72 min, reaction temperature of 106 °C and THF amount of 250 mmol.

described in previous literature [25]. Firstly, glucose would be isomerized into fructose via Lewis acid site derived from ZnO or Al_2O_3. Then, fructose was continuously hydrolyzed into 5-HMF. During this reaction, Bronstated acid site was required with high amount. It should be mentioned here that some intermediate such as ethyl fructose might be formed via ethanolysis and dehydration before formation of HMF product. It may be depended on the selectivity of used catalyst. Finally, EMF product could be easily produced via etherification through a synergistic effect of sulfonic acid and ultrasound. It should be noted that the energy hotspots with gobbet of cavitation bubbles procreated from ultrasound could support mass transfer and interfacial area on the substrate towards a fast reaction rate [26,27]. Meanwhile, inappropriate conditions such as high reaction temperature, too high acidity and long reaction time as well as type of organic solvent resulted in further conversion of EMF into unwanted products such as Humins and polymers. As well known that catalytic conversion of sugar into EMF required high temperature based on endothermic nature. Whereas, the side reaction such as polymerization and carbonization might be occurred in case of too high temperature applied, leading to the reduction of EMF yield [28]. This phenomenon could be observed in the change of color in liquid product from brown color to black color. Considering on economic process, it is possible since all recycle process at short reaction time was well performed and it was acceptable in industrial technology.

The kinetic study of glucose conversion was investigated with a function of reaction temperature and time in the range of 70 to 100 °C and 30 to 70 min, respectively. Here, the optimum catalyst amount (62 mg) and THF amount (250 mmol) were fixed. One can see that glucose conversion favored a first-order reaction as the kinetic data curves in each temperature were well fitted with $R^2 > 0.99$. According to the previous report, Nguyen et al. [29] found that the acid catalyzed glucose dehydration process was a first-order reaction. From the plot of Fig. 8A, the rate constants of 0.0124, 0.0223, 0.0385 and 0.0534 min^{-1} were obtained at 70, 80, 90 and 100 °C, respectively. An increase in the temperature together with rate constant for glucose conversion indicated that high temperature was required for EMF fomation. Moreover, the reaction rate was also supported by cavitation effect from ultrasound, resulting in the creation of microemulsions between the two phases taking part in the reaction, giving faster reaction rates for isomerization, dehydration and etherification processes. Fig. 8B shows the Arrhenius plot of rate constant data controlled at various reaction temperatures. Here, the activation energy and pre-exponential factor were found to be 52.5 kJ/mol and 4.0×10^5 min^{-1}, respectively.

To know more details on catalyst stability for application in practical process, the reusability of SO_3H-Zn-SC and SO_3H-Al-SC were also reused for 5 cycles (Fig. 9). Here, turnover rate (TOR) of glucose conversion to EMF was investigated in each cycle. TOR (min^{-1}) defined by dividing the glucose moles which was converted into EMF per unit of catalyst adding amount and reaction time (mol/g·min) by acid amount of catalyst (mol/g). In addition, glucose conversion was fixed at 50% in order to remove the related parameters such reactant concentrations with various performance of each catalyst. As presented in Fig. 9A, the SO_3H-Zn-SC exhibited excellent reusability for 5 cycles with a few deactivation based on TOR value. This phenomenon should be attributed to leaching of sulfonic and Zn species from catalyst surface. Also, partial blocking of the catalyst pores from adsorption of some reactants during reaction cycle may be one reason for catalyst deactivation [30]. More interestingly, considering on SO_3H-Al-SC, higher performance was found for first cycle, comparing with SO_3H-Zn-SC. Unfortunately, its reusability was quite low. It is probably due to the different of acid sites. It is also possible that larger amount of strong acid sites for SO_3H-Al-SC based on NH_3-TPD results might facilitate for side reaction, leading to the formation of other unwanted product such as EL and humins/polymers. From these results, SO_3H-Zn-SC was expected to further apply for EMF production in practical process.

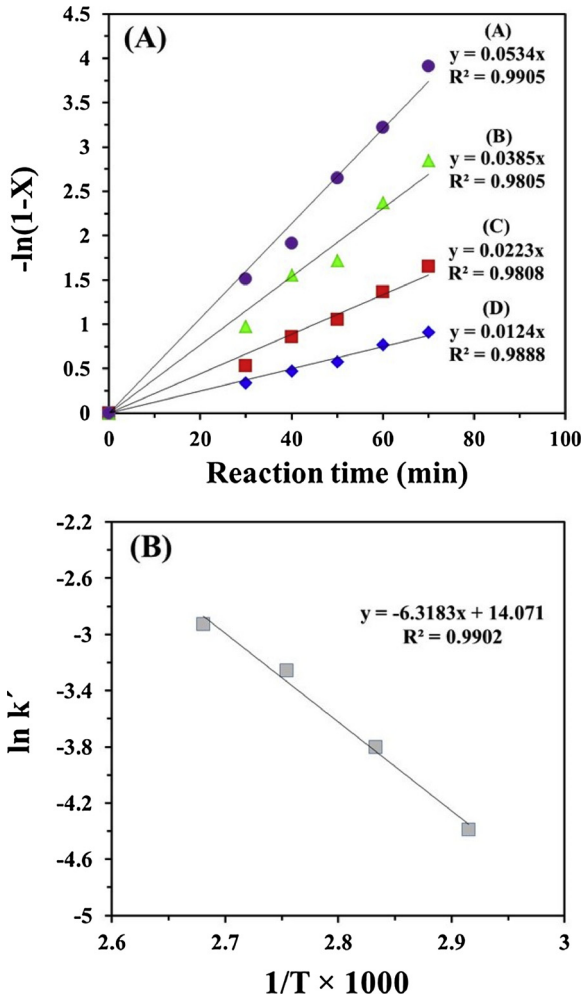

Fig. 8. (A) Plot of –ln(1-X) versus reaction time and (B) Arrhenius plot 1/T versus ln k´ at reaction temperatures of (a) 70 °C, (b) 80 °C, (c) 90 °C and (d) 100 °C.

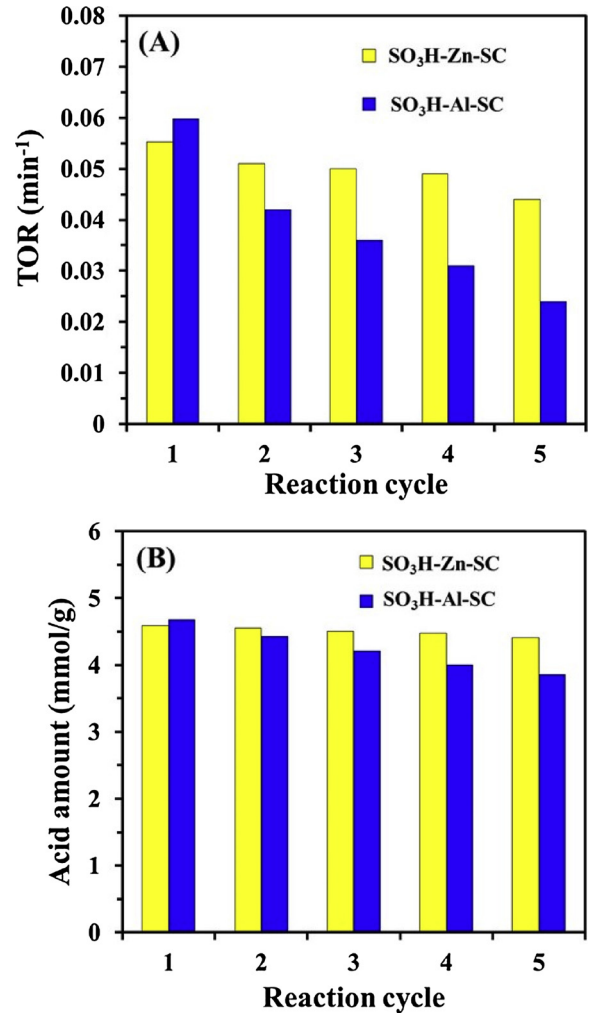

Fig. 9. Reusability obtained from (A) TOR values and (B) acid amount of SO_3H-Zn-SC and SO_3H-Al-SC in each cycle.

Conclusions

The EMF product was easily synthesized with high selectively at short reaction from ultrasonic-assisted transformation of glucose catalyzed by SO_3H-Zn-SC. The EMF yield could be evidently increased from 86.3% to 97.8% when ultrasonic power increased from 70 W to 90 W. This suggested that the higher ultrasonic power well promoted isomerization-dehydration-etherification of glucose. The activation energy and pre-exponential factor for EMF production were found to be 52.5 kJ/mol and 4.0×10^5 min^{-1} A maximum value of TOR (0.06 min^{-1}) was obtained for first cycle. The SO_3H-Zn-SC exhibited excellent reusability for 5 cycles with a few deactivation. This research was expected to further apply in practical process.

Acknowledgments

The authors wish to acknowledge Department of Chemistry, Faculty of Science, Rangsit University for supporting all instruments and chemicals.

Appendix A. Supplementary data

Supplementary material related to this article can be found, in the online version, at doi:https://doi.org/10.1016/j.mcat.2019.110632.

References

[1] J.R. Bernardo, M.C. Oliveira, A.C. Fernandes, $HReO_4$ as highly efficient and selective catalyst for the conversion of carbohydrates into value added chemicals, Mol. Catal. 465 (2019) 87–94.
[2] F. Delbecq, Y. Wang, C. Len, Various carbohydrate precursors dehydration to 5-HMF in an acidicbiphasic system under microwave heating using betaine as a co-catalyst, Mol. Catal. 434 (2017) 80–85.
[3] H. Li, S. Saravanamurugan, S. Yang, A. Riisager, Direct transformation of carbohydrates to the biofuel 5-ethoxymethylfurfural by solid acid catalysts, Green Chem. 18 (2016) 726–734.
[4] M. Zuo, K. Le, Y. Feng, C. Xiong, Z. Li, X. Zeng, X. Tang, Y. Sun, L. Lin, An effective pathway for converting carbohydrates to biofuel 5-ethoxymethylfurfural via 5-hydroxymethylfurfural with deep eutectic solvents (DESs), Ind. Crops Prod. 112 (2018) 18–23.
[5] H. Guo, X. Qi, Y. Hiraga, T.M. Aida, R.L.S. Jr, Efficient conversion of fructose into 5-ethoxymethylfurfural with hydrogen sulfate ionic liquids as co-solvent and catalyst, Chem. Eng. J. 314 (2017) 508–514.
[6] B. Liu, Z. Zhang, K. Huang, Z. Fang, Efficient conversion of carbohydrates into 5-ethoxymethylfurfural in ethanol catalyzed by $AlCl_3$, Fuel 113 (2013) 625–631.
[7] Y. Zhou, S. Niu, S. Li, Activity of the carbon-based heterogeneous acid catalyst derived from bamboo in esterification of oleic acid with ethanol, Energy Convers. Manage. 114 (2016) 188–196.
[8] Z.E. Tang, S. Lim, Y.L. Pang, H.C. Ong, K.T. Lee, Synthesis of biomass as heterogeneous catalyst for application in biodiesel production: state of the art and fundamental review, Renew. Sustain. Energy Rev. 92 (2018) 235–253.
[9] A. Liu, Z. Zhang, Z. Fang, B. Liu, K. Huang, Synthesis of 5-ethoxymethylfurfural from 5-hydroxymethylfurfural and fructose in ethanol catalyzed by MCM-41 supported phosphotungstic acid, J. Ind. Eng. Chem. 20 (2014) 1977–1984.
[10] G. Morales, M. Paniagua, J.A. Melero, J. Iglesias, Efficient production of 5-ethoxymethylfurfural from fructose by sulfonic mesostructured silica using DMSO as co-solvent, Catal. Today 279 (2017) 305–316.
[11] J. Wang, Z. Zhang, S. Jin, Z. Shen, Efficient conversion of carbohydrates into 5-

hydroxylmethylfurfan and 5-ethoxymethylfurfural over sufonic acid-functionalized mesoporous carbon catalyst, Fuel 192 (2017) 102–107.
[12] X. Lin, S. Jei, Z. Liu, Sulfur and nitrogen-doped porous cobalt carbon catalyst for high efficient aerobic oxidation of hydrocarbons, Mol. Catal. 455 (2018) 143–149.
[13] A.V. Nakhate, G.D. Yadav, Cu_2O nanoparticles supported hydrothermal carbon microspheres as catalyst for propargylamine synthesis, Mol. Catal. 451 (2018) 209–219.
[14] K.C. Bedin, A.C. Martins, A.L. Cazetta, O. Pezoti, V.C. Almeida, KOH-activated carbon prepared from sucrose spherical carbon: adsorption equilibrium, kinetic and thermodynamic studies for Methylene Blue removal, Chem. Eng. J. 286 (2016) 476–484.
[15] S.C.L. Dias, J.A. Dias, Effects of the dealumination methodology on the FER zeolite acidity: a study with fractional factorial design, Mol. Catal. 458 (2018) 139–144.
[16] J. Liu, X. Wu, J. Liu, C. Zhang, Q. Hu, X. Hou, Ofloxacin degradation by Fe3O4-CeO2/AC Fenton-like system: optimization, kinetics, and degradation pathways, Mol. Catal. 465 (2019) 61–67.
[17] M. Gonçalves, R. Rodrigues, T.S. Galhardo, W.A. Carvalho, Highly selective acetalization of glycerol with acetone to solketal over acidic carbon-based catalysts from biodiesel waste, Fuel 181 (2016) 46–54.
[18] P. Maneechakr, S. Karnjanakom, Catalytic transformation of furfural into bio-based succinic acid via ultrasonic oxidation using β-cyclodextrin-SO_3H carbon catalyst: a liquid biofuel candidate, Energy Convers. Manage. 154 (2017) 299–310.
[19] S. Karnjanakom, S. Kongparakul, C. Chaiya, P. Reubroycharoen, G. Guan, C. Samart, Biodiesel production from *Hevea brasiliensis* oil using SO_3H-MCM-41catalyst, J. Environ. Chem. Eng. 4 (2016) 47–55.
[20] K. Peng, X. Li, X. Liu, Y. Wang, Hydrothermally stable Nb-SBA-15 catalysts applied in carbohydrate conversion to 5-hydroxymethyl furfural, Mol. Catal. 441 (2017) 72–80.
[21] Y. Wang, F. Delbecq, W. Kwapinski, C. Len, Application of sulfonated carbon-based catalyst for the furfural production from d-xylose and xylan in a microwave-assisted biphasic reaction, Mol. Catal. 438 (2017) 167–172.
[22] P. Maneechakr, S. Karnjanakom, J. Samerjit, Facile synthesis of ZnO particles via benzene assisted co-solvothermal method with different alcohols and its application, RSC Adv. 6 (2016) 73947–73952.
[23] M. Goncalves, C.S. Castro, L.C.A. Oliveira, W.A. Carvalho, Green acid catalyst obtained from industrial wastes for glycerol etherification, Fuel Process Technol. 138 (2015) 695-670.
[24] Y. Zhao, H. Chen, Y. Huang, Y. Zhao, Y. Fu, J. Shen, Sulfonated carbon materials with hydrophilic and lipophilic properties, J. Energy Chem. 23 (2014) 156–163.
[25] Y. Yang, M.M. Abu-Omar, C. Hu, Heteropolyacid catalyzed conversion of fructose, sucrose, and inulin to 5-ethoxymethylfurfural, a liquid biofuel candidate, Appl. Energy 99 (2012) 80–84.
[26] P. Maneechakr, S. Karnjanakom, Selective conversion of fructose into 5-ethoxymethylfurfural over green catalyst, Res. Chem. Intermed. 45 (2019) 743–756.
[27] S. Karnjanakoma, P. Maneechakr, C. Samart, G. Guan, Ultrasound-assisted acetylation of glycerol for triacetin production over green catalyst: a liquid biofuel candidate, Energy Convers. Manage. 173 (2018) 262–270.
[28] S.J. Dee, A.T. Bell, A study of the acid-catalyzed hydrolysis of cellulose dissolved in ionic liquids and the factors influencing the dehydration of glucose and the formation of humins, ChemSusChem 4 (2011) 1166–1173.
[29] C.V. Nguyen, D. Lewis, W.H. Chen, H.W. Huang, Z.A. ALOthman, Y. Yamauchi, K.C.W. Wu, Combined treatments for producing 5-hydroxymethylfurfural (HMF) from lignocellulosic biomass, Catal. Today 278 (2016) 344–349.
[30] H. Yu, S. Niu, C. Lu, J. Li, Y. Yang, Preparation and esterification performance of sulfonated coal-based heterogeneous acid catalyst for methyl oleate production, Energy Convers. Manage. 126 (2016) 488–496.